The correlation of ULF waves and auroral intensity before, during and after substorm expansion phase onset

Article

Published Version

The correlation of ULF waves and auroral intensity before, during and after substorm expansion phase onset

I. Jonathan Rae,[1] Clare E. J. Watt,[1] Kyle R. Murphy,[1] Harald U. Frey,[2] Louis G. Ozeke,[1] David K. Milling,[1] and Ian R. Mann[1]

Received 16 January 2012; revised 4 June 2012; accepted 5 June 2012; published 9 August 2012.

[1] We present case studies of the evolution of Ultra-Low Frequency (ULF) magnetic wave amplitudes and auroral intensity through the late growth phase and the expansion phase of the substorm cycle. We present strong evidence that substorm-related auroral enhancements are clearly and demonstrably linked to ULF wave amplitudes observed at the same location. In all three case studies presented, the correlation analysis shows that the ULF wave activity and auroral intensities are highly correlated at close to zero lag. We discuss four possible explanations that may be able to explain both the timing and the high correlations between these two phenomena, including a simple coincidence, an artifact of instrumental effects, the response of the ionosphere to magnetic waves and auroral particle precipitation, and finally, that ULF waves and auroral particle precipitation are physically linked at their source. We discount coincidence and instrumental effects since we present multiple events where instrumental effects have a negligible contribution, and we find that the ionospheric response to waves and precipitation can explain some, but not all, of the results contained within this paper. Specifically, the ionospheric response to substorm waves and auroral precipitation cannot explain the result backed up by previous studies that the onset of ULF wave activity and the onset of auroral particle precipitation occur at the same time and in the same location. This leaves the possibility that ULF waves and auroral particles are physically linked at their source. We therefore re-emphasize the importance of ULF wave observations in fully understanding the mechanism or mechanisms responsible for rapid auroral brightenings.

Citation: Rae, I. J., C. E. J. Watt, K. R. Murphy, H. U. Frey, L. G. Ozeke, D. K. Milling, and I. R. Mann (2012), The correlation of ULF waves and auroral intensity before, during and after substorm expansion phase onset, *J. Geophys. Res.*, *117*, A08213, doi:10.1029/2012JA017534.

1. Introduction

[2] The physics surrounding the explosive release of energy in the nightside magnetosphere has been a hot topic of study in solar-terrestrial physics for more than sixty years. Traditionally, substorms are defined as the brightening of a pre-existing quiet discrete arc usually in the midnight sector, or in some cases by the formation of a new discrete arc [e.g., *Akasofu*, 1964, 1977]. However, substorms are also closely associated with two magnetic signatures: the presence of a sharp magnetic field deflection or bay, and the commencement of Ultra-Low Frequency (ULF) magnetic wave activity. *Heppner* [1958] demonstrated that the brightening and break-up of the most equatorward arc in the pre-midnight sector was clearly associated with the formation of a sharp magnetic bay in ground magnetometers, which *Angenheister* [1913] noted were associated with geomagnetic pulsations. In an attempt to unify the plethora of categories used to describe these geomagnetic pulsations, *Jacobs et al.* [1964] coined the wave bands "Pi2" (40–150 s period) and "Pi1" (1–40 s period) which, according to both *Jacobs et al.* [1964] and *Saito* [1969] had many similar characteristics. *Saito* [1969] noted that Pi2 pulsations are "long period pulsations which occur essentially at the beginning part of bays" and Pi1 pulsations are "short period pulsations which often occur simultaneously with Pi2," and *Jacobs et al.* [1964] noted that "[u]sually the period of Pi1 is quite small, seldom exceeding 20 sec." and that "[s]ince the physical processes involved are not well understood, it is pointless to introduce a highly sophisticated scheme" when classifying Pi1 and Pi2 ULF wave bands. Combined with their statement that "the boundaries may have to be changed later as further knowledge becomes available" and the lack of justification within the classification scheme for a demarcation between wave bands at 40 s period, it is therefore curious to note that many event studies of substorm-related geomagnetic pulsations have in large part confined

[1]Department of Physics, University of Alberta, Edmonton, Alberta, Canada.
[2]Space Sciences Laboratory, University of California, Berkeley, California, USA.

Corresponding author: I. J. Rae, Department of Physics, University of Alberta, Edmonton, AB T6G 2E1, Canada. (jonathan.rae@ualberta.ca)

0148-0227/12/2012JA017534

themselves to either the Pi2 or Pi1 band, and not considered the entire ULF wave spectrum. Since ULF waves constitute an integral component of a substorm, their characteristics have been used to define many aspects of substorm expansion onset. For example, Pi2s have been used to define the location of the substorm current wedge [e.g., *McPherron et al.*, 1973; *Lester et al.*, 1983], and at low-latitudes to define the meridian of auroral onset [e.g., *Takahashi and Liou*, 2004], and Pi1(B) waves to define the specific region of auroral onset [e.g., *Bösinger and Yahnin*, 1987; *Arnoldy et al.*, 1987; *Bösinger*, 1989]. However, recent work has focused on analyzing the entire ULF wave spectrum spanning both Pi1 and Pi2 bands. Within this recent work, ULF wave power in the long-period Pi1/short-period Pi2 ULF period band has emerged as a robust and repeatable diagnostic for both the time and location of auroral substorm onset, and for other auroral intensifications [e.g., *Milling et al.*, 2008; *Mann et al.*, 2008; *Murphy et al.*, 2009a, 2009b; *Rae et al.*, 2009a, 2009b, 2010; *Walsh et al.*, 2010].

[3] As with all aspects of substorm research, controversy remains as to how to routinely determine the onset of specific features in the ionosphere, as well as in the magnetosphere (see, for example, the recent debate between *Angelopoulos et al.* [2008], *Lui* [2009], and *Angelopoulos et al.* [2009]). Perhaps one of the major drawbacks with studying substorm onset lies in how to define the onset of features that by definition are subject to exponential growth. A number of studies have attempted to relate an onset of ULF wave activity to auroral onset but these studies typically have either attempted to visually identify the onset of ULF wave activity [e.g., *Liu et al.*, 2011], or constructed an onset criterion based upon the maximum observed ULF wave amplitude [e.g., *Liou et al.*, 2000]. A further complication arises from analyzing ULF wave activity and auroral intensities from differing locations; that is, comparing the location of auroral onset with the clearer ULF wave signatures observed at lower latitudes. Since there is a delay between signals observed at the auroral zone and those at lower latitudes based upon travel time magnetoseismology [e.g., *Uozumi et al.*, 2000; *Chi et al.*, 2009], this would add even more uncertainty in the relative timing of the growth of ULF wave amplitudes and auroral intensities (see, for example, *Liou et al.* [2000] and comments by *Kepko and McPherron* [2001]).

[4] To complete the inter-relationship of the ionospheric signatures of substorm onset, recent work has also focused on broadband electron precipitation during substorms. This broadband electron signature has been shown by *Mende et al.* [2003] to be consistent with signatures of wave-driven auroral acceleration [e.g., *Chaston et al.*, 2000; *Watt et al.*, 2005]. Recently, *Newell et al.* [2010] presented evidence that this broadband electron precipitation is significantly enhanced at, or indeed slightly in advance of, auroral onset and persists for at least 15 min following onset.

[5] Since it is clear that auroral intensifications, geomagnetic bays and ULF waves are three necessary criteria that together constitute the ionospheric signatures of substorm expansion phase onset, without which no substorm is complete, then it is logical to try and determine the interdependency between these specific signatures. Rather than limit the study of substorm onset to one instant in time, this study seeks to understand the physics of the onset process throughout a period that contains the onset time. Here, we concentrate on the relationship of the growth of auroral intensity and the growth of ULF wave amplitudes through a period of many minutes which definitively contains expansion phase onset, to clearly understand the relationship of two of the three exponentially growing signatures that accompany auroral substorm onset.

2. Data and Methodology

[6] We select events that fulfill two basic criteria: where a clear auroral brightening was captured close to the center of any THEMIS ASI field-of-view, and where co-located ground magnetometer data was available throughout the event. Although the co-located ground magnetometers integrate the magnetic signatures from all currents flowing in the overhead ionosphere on scales of $\sim$100 km, these criteria ensure that both magnetometers and ASIs have as similar a viewing area as possible for the subsequent quantitative analysis. We further limit events to those whereby the intensity recorded by the THEMIS ASI did not saturate for at least 10 min following onset, and so a true representation of the auroral intensities could be captured.

[7] We use the Automated Wavelet Estimation of Substorm Onset and Magnetic Events (AWESOME) [*Murphy et al.*, 2009a] to extract the ULF wave amplitude time series from the magnetometer time series. No quiet time baseline estimates have been subtracted and so each wavelet time series represents wavelet-filtered ULF wave power as a function of time through each auroral expansion. Time series of the measured ASI intensities within a latitudinal and longitudinal region that is defined to encompass both the onset arc and the region into which the auroral surge develops are extracted and summed in order to compare the time series of auroral intensities with the time series of ULF wave amplitudes. In the following section we detail the correlation between the growth of auroral intensities and the growth of magnetic wave amplitudes before, during and after substorm onset.

3. Results

3.1. The 5 March 2008 Event

[8] This event was first reported on by *Liu et al.* [2008]. In their paper, *Liu et al.* [2008] identified the intensification of the break-up arc at around 0604 UT from the CGSM GILL Multi Spectral Imager (MSI) green line emissions. Here, we use the THEMIS ASI data at GILL to monitor the white light auroral intensity as discussed in section 2.

[9] Figure 1 shows the ground magnetometer and ASI data from the GILL CARISMA [*Mann et al.*, 2008] magnetometer and the THEMIS ASI [*Mende et al.*, 2008] for 5 March 2008 from 0530 to 0700 UT. Figure 1 (top) shows a keogram that is computed in a direction perpendicular to the break-up arc, and off zenith, in the region where *Liu et al.* [2008] first identify onset in the GILL MSI. Figure 1 (middle) shows the H, D, and Z component magnetic fields at GILL, and Figure 1 (bottom) shows a time sequence of 2-D auroral images that surround the onset of the auroral expansion from 0600 to 0608 UT for context, including the

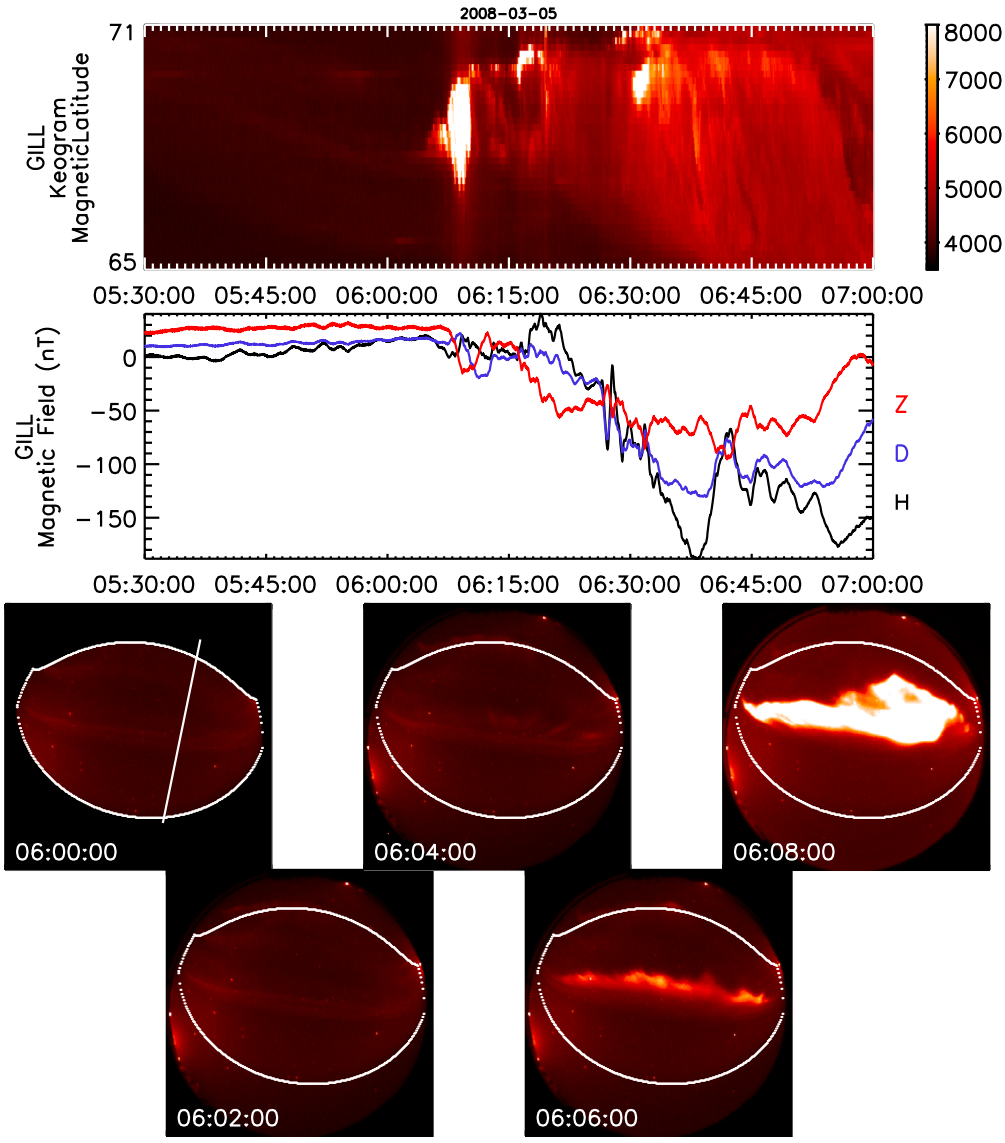

Figure 1. (top) A time series of north-south cuts through the THEMIS ASI data from the GILL station (keogram) in a direction perpendicular to the break-up arc orientation and (middle) H-, D- and Z-component magnetic field from the CARISMA GILL magnetometer from the 5th March 2008 0530–0700 UT. (bottom) Raw ASI images over the period spanning the first initial brightening shown in the keogram at 2-min intervals. The white line shown in the first panel represents the longitude and orientation of the keogram shown above, which corresponds to the longitude that first displays the detectable auroral signatures along the break-up arc, and the white box denotes the latitudinal and longitudinal region over which the auroral intensities are summed for analysis (see text for details).

region limited by lines of constant magnetic latitude and longitude from which the summed ASI intensities are extracted, from 66 to 69° latitude and −5 to −55° longitude (as shown by the white boundary). *Liu et al.* [2008] described this event as a small substorm, although it most closely resembles a pseudo-breakup; that is, the arc intensifies and progresses poleward, but no real break-up is shown, and the largest ground magnetic signatures of a substorm develop much later in the interval (cf. Figure 1). Within the first few minutes of auroral onset, a clear auroral undulation can be seen along the onset arc [e.g., *Liang et al.*, 2008; *Sakaguchi et al.*, 2009; *Rae et al.*, 2009a, 2009b, 2010].

[10] The basis of the AWESOME algorithm expounded by *Murphy et al.* [2009a] is the utilization of the Meyer wavelet transformation. The Meyer wavelet transformation decomposes a time series into n period bands, where the time series is 2^n in length. Each period band in the Meyer wavelet encompasses

$$\frac{3 \times 2^n}{2^{j+2}} \leq T \leq \frac{3 \times 2^n}{2^j} \quad (1)$$

The determination of period bands of 6–24 s, 12–48 s, 24–96 s and 48–192 s is therefore constrained by the

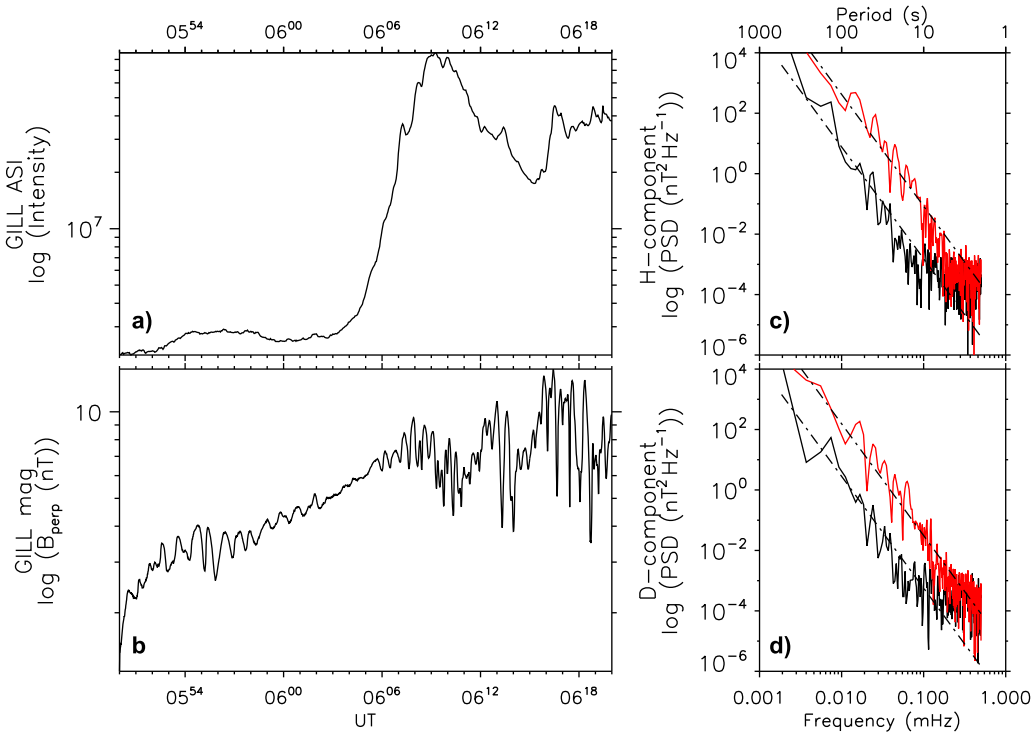

Figure 2. (a) Total counts observed by the THEMIS GILL ASI as a function of time, together with (b) the wavelet-filtered 1–192 s transverse ULF pulsations during the 0550–0620 UT period. The panels on the right represent (c) H-component and (d) D-component ULF wave power spectral densities from pre- and post-onset (denoted by the black and red lines, respectively). The dashed lines on both Figures 2c and 2d represent the gradient of power law calculated by *Murphy et al.* [2009a] with exponent of −3.7, determined statistically during the 40-min period surrounding auroral onset, for reference.

construction of the wavelet basis function, rather than having any physical basis. However, these wavelet bands approximately span period bands within the Pi1 and Pi2 frequency ranges, with minimal overlap in frequency (see *Murphy et al.* [2009a] for details). Additionally, larger (smaller) period bands have low (high) temporal resolution, but high (low) frequency resolution. Figure 2 shows the auroral intensity from the THEMIS GILL ASI, together with the summed (6–192 s period) Meyer wavelet filtered H- and D-component transverse amplitudes over the Pi1 and Pi2 frequency ranges. Figure 2 also shows the Power Spectral Densities in the H- (Figure 2c) and D-component (Figure 2d) magnetic fields in the pre- (black) and post-onset (red) intervals. The power law with exponent of −3.7 found by *Murphy et al.* [2009a] to be observed during a 40-min period centered upon substorm onset is superposed upon the graph, and an arbitrary intercept is applied for pre- and post-onset ULF wave activity to aid the eye. Clear from Figure 2 is that the auroral intensities and large-scale ground magnetic field fluctuations are suppressed before ∼0604 UT, and increase substantially following ∼0604 UT. This can be seen in both the time series and the ∼decade increase in PSD shown pre- and post-0604 UT. However, a recent literature of work has shown that ULF wave amplitudes at different frequencies have different onset times [e.g., *Milling et al.*, 2008; *Mann et al.*, 2008; *Murphy et al.*, 2009a, 2009b; *Rae et al.*, 2009a, 2009b, 2010; *Walsh et al.*, 2010]. In the following section, we show that the growth of waves amplitudes is also frequency dependent by separating this frequency band into different frequencies. Figure 3 (top) shows the wavelet amplitudes (on an arbitrary scale) split into their constituent period bands of 6–24 s, 12–48 s, 24–96 s and 48–192 s. For brevity, we will refer to these period bands by their central period where the amplitudes maximize, which are 8 s, 16 s, 32 s and 64 s, respectively. Clear from Figure 3 is that ULF wave amplitudes are very dependent on the period band studied, typical of any power law, but the general trends and order of magnitude increases are remarkably similar surrounding auroral onset. There are noticeable differences in the time series away from auroral onset in, for example, the 64 s period band which increases at a time closely coincident with the increase in auroral intensity, but also increase ∼10 min prior to this time. For the shorter period wave bands, it appears that these waves are primarily associated with the growth of auroral intensities surrounding onset.

[11] Figure 3 (bottom) shows the correlation coefficients of the amplitudes of each of the wavelet period bands with the ASI intensities during the period of exponential growth, 0600–0610 UT. A maximum lag that is less than zero corresponds to the wavelet amplitudes and ASI intensities being best correlated when the magnetometer time series is moved forward in time, and vice versa for a positive lag. During this event, it is clear that there are large correlations approaching 0.90 for all four ULF wave bands for lags close to zero. These maximum correlations occur within 1 min of a zero lag, ranging from −63 s for the 32 s, −54 s for the 64 s, 0 s lag for the 8 s, and finally +24 s for the 16 s period band. We note that the AWESOME wavelet technique has a period-

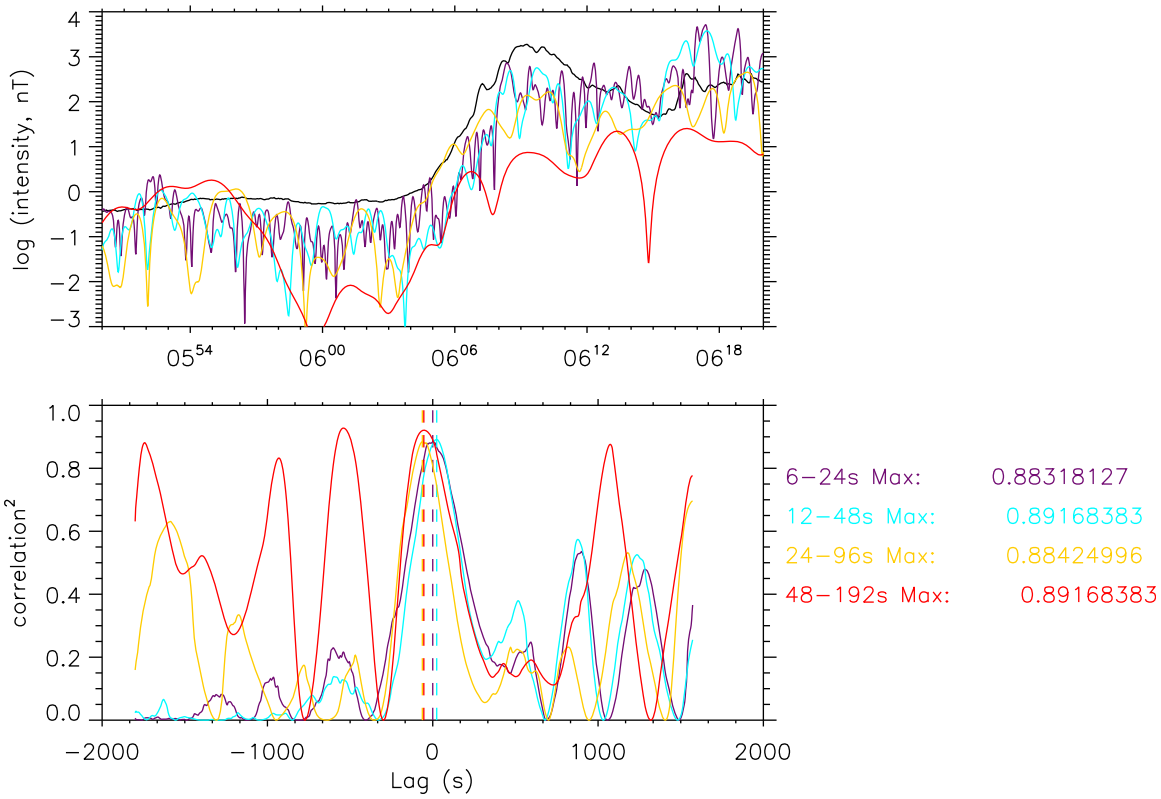

Figure 3. (top) Wavelet-filtered ground magnetic amplitudes in the 6–24, 12–48, 24–96, and 48–192 s ULF wave bands, together with the ASI intensity shown in Figure 2a. (bottom) Correlation coefficients of the amplitudes of each of the wavelet period bands with the ASI intensity as a function of relative lag during the period of exponential growth, 0600–0610 UT.

dependent timing uncertainty. At ULF wave frequencies, the uncertainties are ±32 s for the 64 s, ±16 s for the 32 s, ±8 s for the 16 s, and ±4 s for the 8 s period bands. No other uncertainty is introduced into cross-correlation lag analysis. Hence, we can only estimate that the growth of 32 s and 64 s band ULF waves are observed in advance of the auroral intensities. It should be noted, however, that there are large correlations throughout the interval between the ASI intensities and the 64 s period band, suggesting that exponential increases in wave amplitude in the 64 s period band are not limited to auroral onset, at least in the localized region corresponding to the GILL ASI. Note that Figure 3 (bottom) also relative time delays between the growth of wave amplitudes at different frequencies, which serves to smear out the behavior of the magnetic wave amplitudes if a coarser band-pass filter is used.

[12] In summary, the growth and evolution of THEMIS ASI intensities and ground magnetic wave amplitudes are intimately linked during this event.

3.2. The 11 March 2008 Event

[13] The auroral intensification displayed during this event represents the intensification of an auroral arc during a more classical substorm onset. Figure 4 shows the summary of the 11 March 2008 event from 0530 to 0630 UT in the same format as Figure 1, and the region over which we sum the intensities for this event is from 62 to 71° magnetic latitude and −30 to 25° longitude (as shown by the white boundary in Figure 4 (bottom)). Following an enhancement in the directly driven current systems at ∼0550 UT, a clear and sharp auroral brightening and substorm-like magnetic bay is seen in the SNKQ ASI and magnetometer around 0554 UT, upon which are superimposed large-amplitude (up to 100 nT peak-to-peak) ULF pulsations.

[14] Figure 5 shows the wave amplitudes and correlation coefficients across the 0530–0610 UT interval, in the same format as Figure 3; for 8, 16, 32 and 64 s central periods. High correlations ($c^2 > 0.8$) are observed close to the auroral intensification, and are highest in the lowest period band. All correlations between ULF period bands and ASI intensities peak at negative lags. This clearly demonstrates that, in this case, the best correlations occur when the magnetometer time series are advanced in time i.e., when magnetometer pulsations leads ASI intensities. Note that the 64 s period band has a maximum correlation at lag of ∼−900 s, which is most likely due to the previous increase in ASI intensities around ∼0541 UT, and is hence unrelated to this particular event study, and the closest and highest correlation coefficients in the 64 s period band are smaller (∼0.75) and at a lag of ∼−80 s. The shorter period bands are highly correlated at closer lags (see Table 1). It should again be noted that there are high correlations of the longer wave period bands at lags far from the auroral intensification studied (e.g., in the 64 s period band), whereas the higher correlations in the shorter period bands are seen to fall away from the initiation time of auroral intensity in the ASI. Once

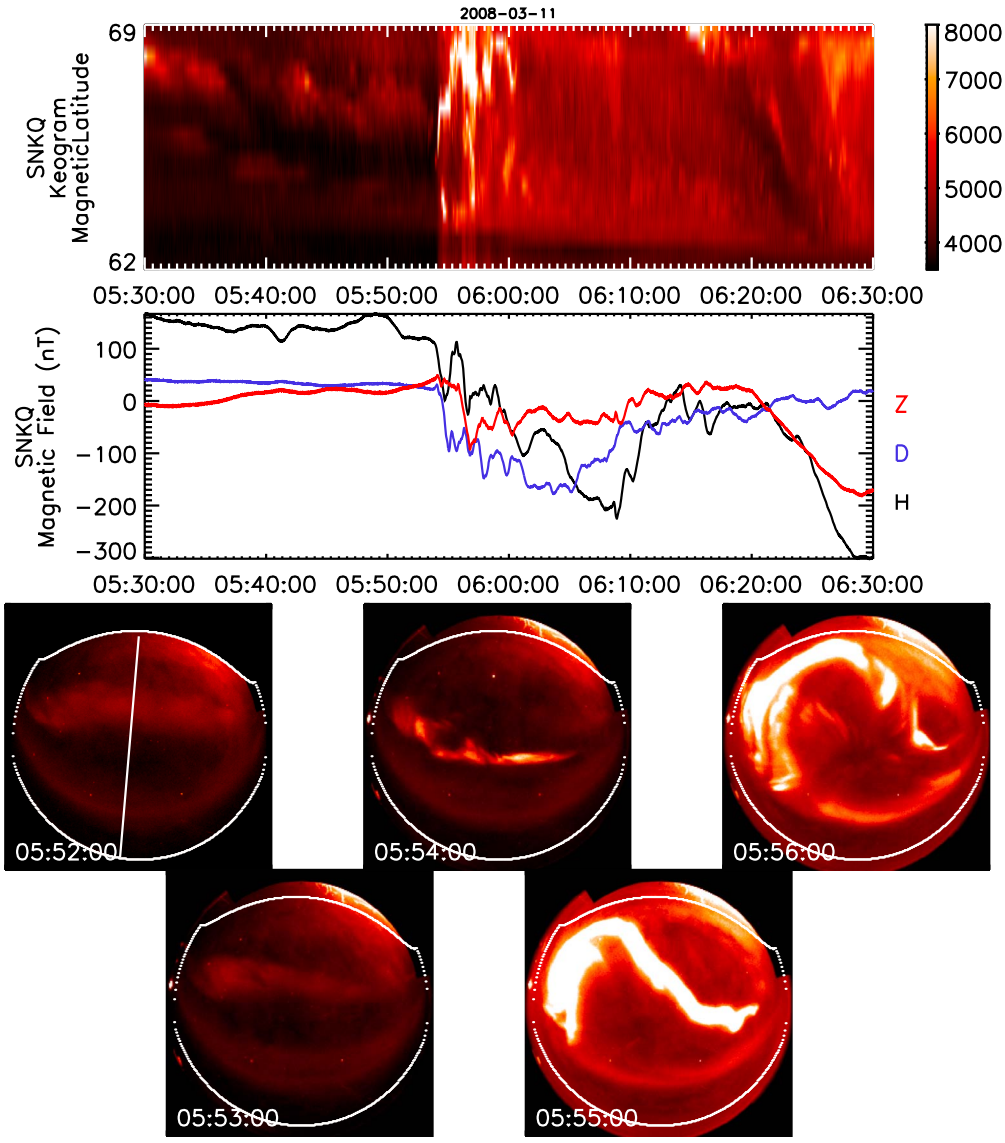

Figure 4. (top) A keogram from the THEMIS GILL; (middle) H-, D- and Z-component magnetic field from the CARISMA GILL magnetometer from the 11th March 2008 0530–0630 UT; and (bottom) raw ASI images over the period spanning the first initial brightening, in the same format as Figure 1.

again, we summarize that the growth and evolution of THEMIS ASI intensities and ground magnetic wave amplitudes are intimately linked during this event.

3.3. The 12 March 2010 Event

[15] In sections 3.1 and 3.2, we demonstrated that small, isolated auroral intensifications and ULF waves are intimately, and demonstrably, linked. The AWESOME-derived magnetometer time series, split into arbitrary ULF wave bands, is highly ($c^2 > 0.81$) correlated with the intensities recorded from the THEMIS ASIs. In this event, we study a two-step auroral intensification on 12 March 2010, in order to investigate whether this relationship is ubiquitous to multistep auroral intensifications, or only seen in isolated cases.

[16] Figure 6 shows a keogram, magnetometer time series and 2D ASI summaries from the SNKQ THEMIS ASI and CANMOS magnetometer, in the same format as Figure 1 over the 66–70° latitudinal range and −20 to +10° longitudes. Within the initial auroral brightening around 0416 UT, small, negative H and Z magnetic field deflection are seen, indicative of an increase in the westward electrojet. In the full substorm occurring shortly after 0422 UT, a clear negative H-component can be seen, closely coincident with the undulation, brightening and subsequent break-up of the auroral arc into a surge-like form. Clear again are reasonably large ULF wave signatures in the H-component time series. Using the substorm current wedge model outlined by *Smith et al.* [2002], a large negative H-component, positive D-component and negative Z-component means that the SCW central latitude is slightly poleward of the SNKQ station and the central longitude slightly to the east, SNKQ being situated close to the upward FAC region. Shortly after 0440 UT, another auroral intensification occurs, closely coincident with a large positive deflection of the

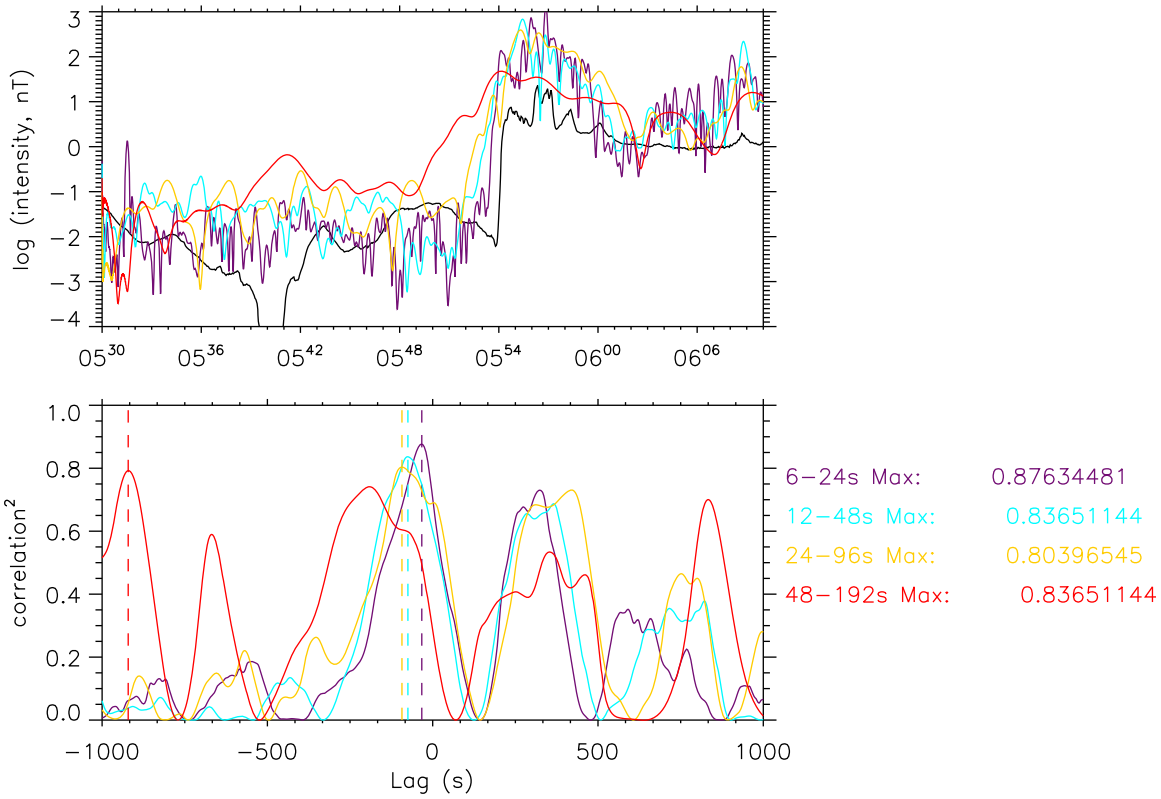

Figure 5. (top) Wavelet-filtered ground magnetic amplitudes and ASI intensity shown in Figure 4 and (bottom) correlation coefficients as a function of relative lag during the two periods of exponential growth, 0415–0425 UT, in the same format as Figure 3.

H-component magnetic field, a slight positive deflection of the Z-component and a small negative deflection of the D-component follows several minutes later. This suggests that a new activation has occurred somewhat equatorward and to the east of SNKQ according to the *Smith et al.* [2002] model. Since this means that the first signature of this auroral activation may not be seen in the SNKQ ASI, we concentrated on the first two intensifications.

[17] The increase in auroral intensities and wavelet powers are shown in Figure 7, in the same format as Figure 3. Correlation coefficients were computed over the two step intensification between 0415 and 0425 UT, in order to verify whether ULF wave amplitude was associated with both auroral intensifications recorded, and not just simply the explosive auroral growth associated with the substorm. It can clearly be seen that there are high correlations across a wide range of both positive and negative lags in this multistage event. For example, the 64 s period band is most highly correlated with ASI intensities at lags of ∼−200 s. Note that this correlation peak does not correspond to the inter-intensification time of ∼400 s as shown in Figure 7. However, since all four ULF wave bands have a high correlation peak ($c^2 > 0.8$) at a time which is closely coincident to the increase in ASI intensities (within timing uncertainties), it can be seen that the growth of ULF waves and auroral intensities are related across more than one activation.

[18] It should be noted, however, that a visual inspection of the ULF and ASI time series is required to reliably interpret the correlative analysis. From the time series, it can appear as if the magnetometer power leads the optical intensity by a

Table 1. Correlation Coefficients (Squared) and Their Respective Lag Between the ASI Time Series and the Magnetometer ULF Amplitude Time Series[a]

	2008-03-05 0600–0612 UT		2008-03-11 0550–0600 UT		2010-03-12 0415–0424 UT (0420–0424 UT*)	
Wave Band	Lag (s)	Correlation^2	Lag (s)	Correlation^2	Lag (s)	Correlation^2
48–192 s (64 s)	−54	0.92	−91	0.79	−195	0.89 (N/A*)
24–96 s (32 s)	−63	0.88	−93	0.80	+42	0.87 (0.96*)
12–48 s (16 s)	+24	0.89	−75	0.83	+27	0.82 (0.90*)
6–24 s (8 s)	0	0.88	−33	0.88	+12	0.69 (0.84*)

[a]A high coefficient and positive lag implies that the magnetic time series occurs later than the ASI time series, and a high coefficient and negative lag implies that the magnetic time series shows exponential growth prior to the ASI time series. The brackets and asterisk denote the correlation coefficients computed again for the multistep auroral intensification, but limited to the substorm intensification only.

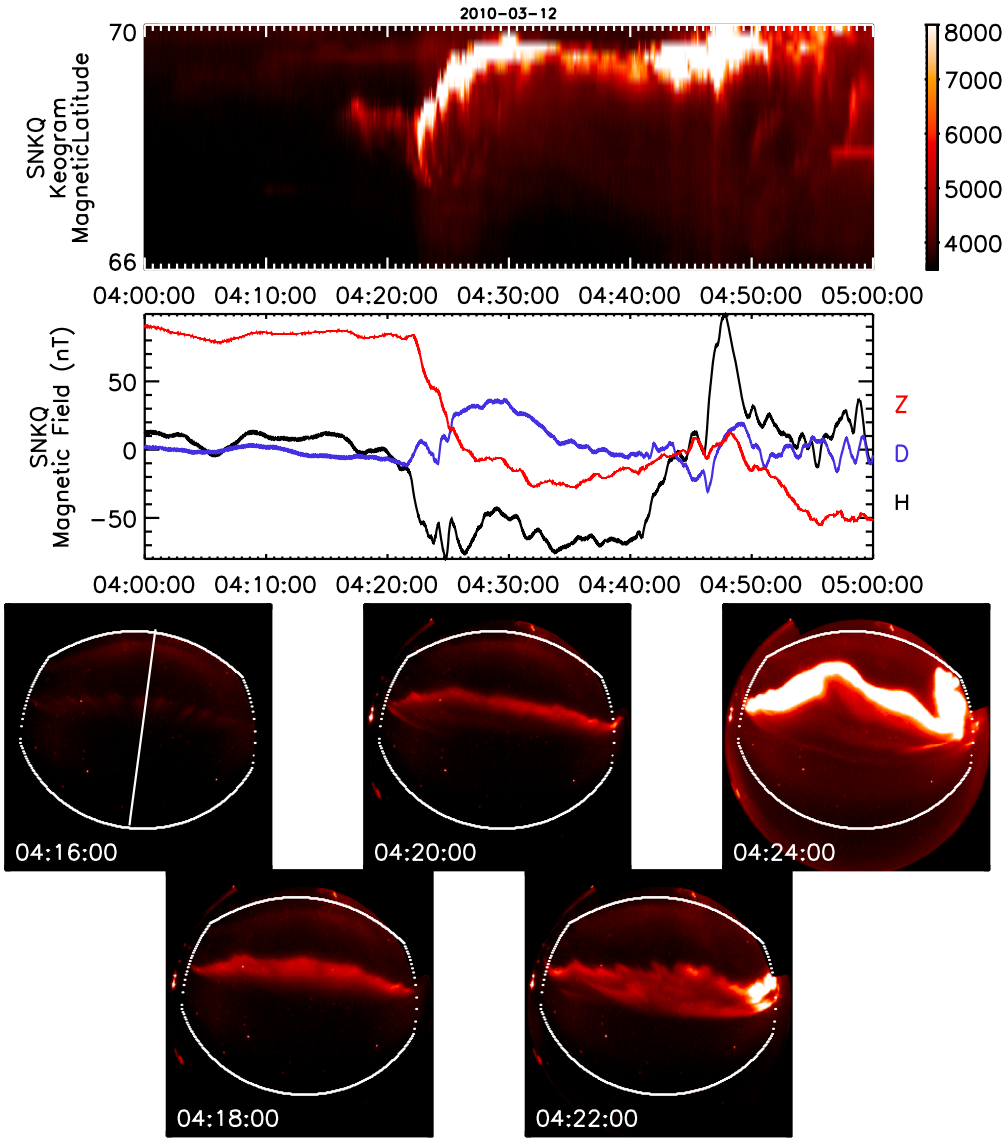

Figure 6. (top) A keogram from the THEMIS SNKQ; (middle) H-, D- and Z-component magnetic field from the CANMOS SNKQ magnetometer from the 12th March 2010 0400–0500 UT; and (bottom) raw ASI images over the period spanning the first initial brightening, in the same format as Figure 1.

few tens of seconds, since its absolute value lies above the optical intensity, but this could be due to the common scale in Figure 7. A median amplitude/intensity is removed from each time series in order to look at the relative changes in amplitude/intensity, and so it is important to consider the shape of each time series, rather than its vertical position in Figure 7. If the reader concentrates on the two intensifications independently (i.e., 0416–0418 UT and 0422–0426 UT), then the start of the shorter period ULF wave growth is almost contemporaneous with the ASI intensity growth.

[19] What is clear again is that the growth of auroral intensities and the evolution of ULF wave amplitudes are clearly linked during this two-stage auroral brightening and substorm.

4. Discussion

[20] We consider four possible general explanations as to why ULF waves and auroral intensities correlate extremely well through substorm-like auroral intensifications. These are coincidence, an instrumental effect, ionospheric response to magnetic wave and particle precipitation, and that the waves and particles may actually be physically related at their source. We discuss these in order of least likely to most likely.

[21] First, we discuss the possibility that growths of ULF waves and auroral intensities are coincidental. In this paper, we show that three arbitrarily selected case studies show a high correlation of the growth of ULF wave amplitudes and auroral intensities. Although this is not an exhaustive analysis, we must still consider that these three case studies may not be typical events, and so we cannot completely rule out coincidence. However, in an independent study, *Rae et al.* [2011] investigated ~250 auroral intensifications and demonstrated statistically that ULF wave amplitudes underwent exponential growth during an interval encompassing independently defined auroral onset times [e.g., *Nishimura et al.*,

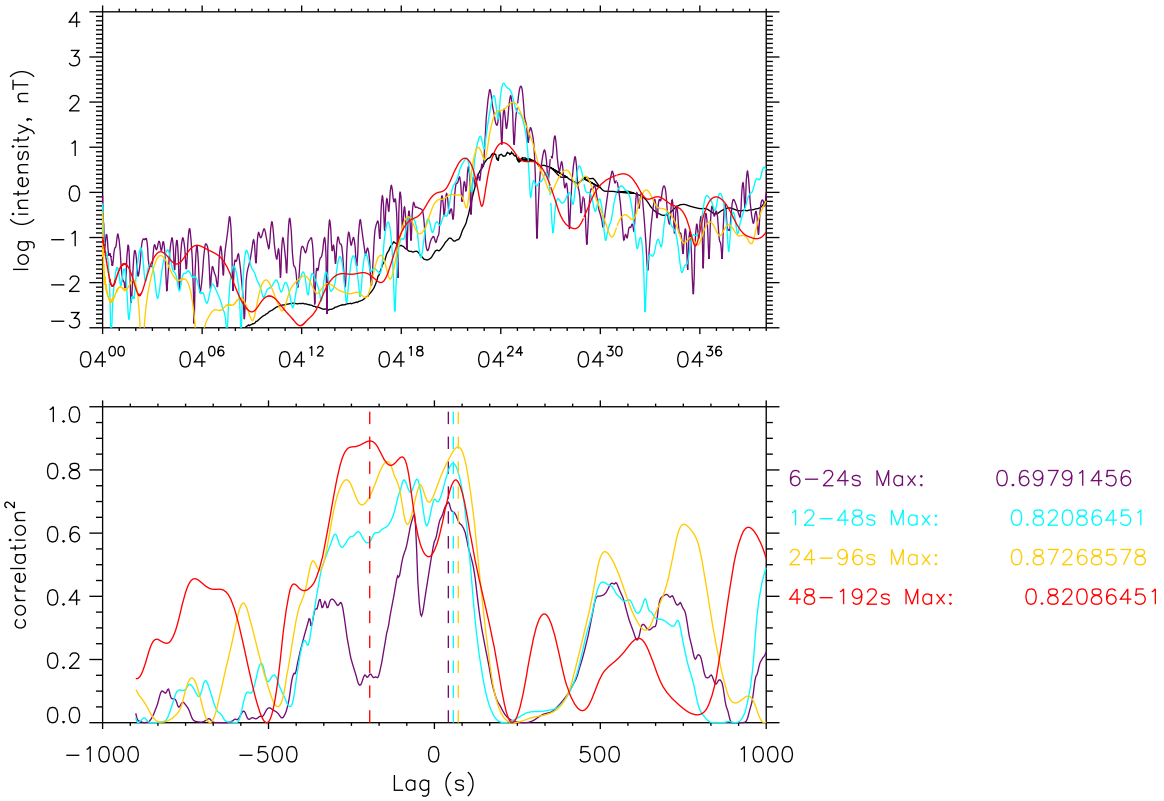

Figure 7. (top) Wavelet-filtered ground magnetic amplitudes and ASI intensity shown in Figure 6 and (bottom) correlation coefficients as a function of relative lag during the two periods of exponential growth, 0415–0425 UT, in the same format as Figure 3.

2010]. Given that auroral onset is by definition an increase in auroral intensity, we therefore find that there is little evidence for this relationship being one of simple coincidence.

[22] Second, although not considered to be a primary reason for the high correlation, we should also consider that instrumental effects may play some role in the detection of the growth of ULF wave amplitudes prior to the growth of auroral intensity. *Mende et al.* [2008] showed that it is essentially impossible to determine the precipitating energy input from the white-light ASIs. *Mende et al.* [2011] went on to show that each THEMIS ASI recorded a slightly different count rate and intensity, for a given 100 kR input. This may contribute to the timing of the growth of ASI intensities at differing stations, but would not contribute to the high correlation during the period of growth. Therefore, a given ASI may not be as sensitive as another ASI to, for instance, soft electron precipitation. If ULF wave growth and ASI intensities are indeed physically linked at their source, then if there are instrumental effects it should be expected that the lag between their respective growths should be station-dependent. However, to a first order, this sensitivity is similar across all THEMIS ASIs (S. Mende, private communication, 2011), and so is not likely to significantly impact the relative timing of ASI intensity and ULF wave growth. Irrespective of this, the relative sensitivity of the ASIs does not play a role in the high correlation between auroral intensity and ULF wave characteristics.

[23] Third, we must consider that the response of the ionosphere to ULF waves and auroral particle precipitation may play a role in this relationship of ULF waves measured with ground based magnetometers, and auroral intensities. These effects can be further categorized into three subconsiderations: ionospheric conductivity effects, ionospheric screening and ionospheric damping.

[24] *Ionospheric conductivity effects.* We assume that some fraction of the transverse pulsation amplitudes on the ground are at due to shear Alfvén waves incident on the ionosphere and not at the critical conductance such that at least part of their amplitude is transmitted through the ionosphere. In this case, the amplitude of ULF pulsations observed with ground-based magnetometers produced by shear Alfven waves is proportional to the ratio of the height integrated Hall conductivity Σh over the height integrated Pedersen conductivity Σp, [e.g., *Hughes and Southwood*, 1976; *Glassmeier and Junginger*, 1987; *Yoshikawa and Itonaga*, 2000]. One possible explanation for the observed coincidence of ground magnetometer pulsations with auroral intensity is that in the auroral region, the ratio of $\Sigma h/\Sigma p$ is enhanced resulting in an enhancement of the pulsations in the auroral region measured on the ground. In short, there may be a pre-existing low amplitude background spectrum of ULF waves, and during the auroral onset the observed ground magnetometer pulsations below the auroral region are enhanced due to an increase in the ratio of $\Sigma h/\Sigma p$. In this hypothesis, ULF waves could then be ubiquitous and constitute either a background magnetospheric state, or else ULF waves are observed before auroral onset in all cases, and it is simply the increase in auroral precipitation that

allows these waves to be "seen." However, although both Σh and Σp increase during a substorm, the ratio remains close to unity [e.g., *Lester et al.*, 1996]. Therefore, we must discount the effects of ionospheric conductivity as being a primary driver for the relationship between waves and particle precipitation presented in this paper.

[25] *Ionospheric screening.* Recently, periodic structuring of substorm onset arcs has received a significant amount of attention in the literature, primarily because of the increased temporal and spatial resolution available via the THEMIS ASIs throughout an extended region of the northern hemisphere [e.g., *Donovan et al.*, 2008; *Liang et al.*, 2008; *Sakaguchi et al.*, 2009; *Rae et al.*, 2009a, 2009b, 2010]. *Sakaguchi et al.* [2009] found that, in some cases, the increase in auroral intensities occurred in a series of localized regions (~30–60 km) with a longitudinal wavelength of ~100 km. *Rae et al.* [2010] demonstrated clearly that the temporal evolution of the azimuthal undulations along a substorm onset arc initially formed at azimuthal spatial scales of ~70 km (which corresponds to azimuthal wave numbers of m~250), before evolving to larger spatial scales in excess of 100 km (as first reported by *Friedrich et al.* [2001]). It should be noted that small-amplitude ULF waves have been observed at the same time and at the same location as the first observable signatures of auroral onset [e.g., *Rae et al.*, 2009a, 2009b, 2010; *Walsh et al.*, 2010]. This raises the interesting possibility that the ULF wave activity may be partially screened from ground magnetometers due to their large m, but once these small scales evolve into larger scales, the ULF wavefields would be detected on the ground. However, since *Rae et al.* [2009a, 2010] also demonstrated that the onset of ULF wave activity was co-located in both time and space with the onset of auroral fluctuations, it would suggest that this effect is not important.

[26] *Ionospheric damping.* The reflection coefficient of shear Alfvén waves from the ionosphere depends on the height integrated Pedersen conductivity. If the Pedersen conductance is equal to a critical value, Σpc, then all of the waves' energy is absorbed by the ionosphere and the reflection coefficient is zero. However, away from the critical value Σpc, then an impedance mis-match will allow traveling Alfvén waves to be either reflected or transmitted depending upon whether Σp is higher or lower than Σpc. Typically, on the nightside of the ionosphere, the Pedersen conductance is close to the critical conductance causing the waves to be highly damped on the nightside [see *Newton et al.*, 1978]. However, on the nightside ionosphere in the auroral zone the waves may still be reflected from the ionosphere due to the enhanced Pedersen conductivity there. Due to the reflection of the waves from ionosphere in the auroral zone, large amplitude standing waves could be produced at certain frequencies on the nightside. However, these large amplitude standing waves are not predicted to occur at exactly the same time as the auroral onset but would be produced multiple wave bounce periods later. Since these observations show that the relationship between ULF wave amplitudes and auroral intensities is closely coincident in time, then we should also rule this effect out as being a primary driver for the relationship between particles and waves.

[27] Our fourth candidate for the linkage of ULF waves and particle precipitation is that the waves and particles are physically linked at their source. If the growth of ULF wave amplitudes and auroral intensities are physically linked in the magnetosphere or upper atmosphere, then these observations potentially represent a powerful diagnostic of the magnetospheric physics of substorm onset. However, a single point measurement cannot distinguish causality and we are left with three scenarios whereby the waves and particle precipitation are linked. First, it is possible that the precipitating (field-aligned) electron beams and their associated velocity shears drive ULF waves unstable [e.g., *Asamura et al.*, 2009, and references therein]. In this scenario, gradients in electron motion perpendicular to the field and within the shear flow across an auroral arc can generate low-frequency ULF waves [e.g., *Peñano and Ganguli*, 2000; *Wu and Seyler*, 2003]. Second, it is also possible that the precipitating particles and ULF waves have a common source in the magnetosphere. This common source could be reconnection whereby Alfvén waves [e.g., *Shay et al.*, 2011] and accelerated electrons are both launched by the reconnection region, or the source could be a near-Earth plasma instability [e.g., *Voronkov et al.*, 1997; *Friedrich et al.*, 2001]. The final mechanism with perhaps the most published literature associated with it, is that ULF waves in the form of shear Alfvén waves with small perpendicular scales, can accelerate electrons in the field-aligned direction to produce precipitation. This acceleration could take place in the warm plasma of the plasma sheet [e.g., *Wygant et al.*, 2002; *Watt and Rankin*, 2009], in the "auroral acceleration region" [e.g., *Chaston et al.*, 2002], or in the Ionospheric Alfven Resonator (IAR) [e.g., *Lysak*, 1991].

[28] There are two subtle wrinkles in the applicability of these hypotheses to the observations presented in this paper. First, if ULF waves with short perpendicular scales are indeed responsible for the increase in auroral intensity, then by definition, these waves will have surrendered their energy to the precipitating electrons, and would not be observed on the ground. However, it is not necessarily the case that the waves will convert all their energy to particle acceleration. *Dombeck et al.* [2005] showed that only half of the field-aligned Poynting vector at 6–7 R_E was converted into auroral electron energy flux by the time the waves reached $0.5R_E$ altitude. If there is further interaction between the waves and the particles below 0.5 R_E (not investigated in *Dombeck et al.* [2005]), then there may be little wave power left at the ionosphere to be observed using ground-based magnetometers. If, on the other hand, the acceleration process is complete at high-altitude, then there may be sufficient ULF wave power reaching the ionosphere to account for the observations presented here. Second, *Dombeck et al.* [2005] also showed that the damping of the ULF wave Poynting vector is frequency-dependent. That is, only ULF waves of specific frequencies showed significant reduction in wave energies between 6 and 7 R_E and 0.5 R_E. This raises the possibility that the ULF waves observed on the ground may be part of a continuum of broadband energy launched from a magnetospheric source, and that those ULF waves that are observed by ground-based magnetometers are simply those waves in the continuum which did not have the short perpendicular scale lengths required to acceleration electrons.

[29] The relationship of ULF wave activity to the particle precipitation that is captured by a measurement of auroral intensities may involve a complex and indirect route that relies on a number of stages of acceleration that cannot be resolved with ground-based measurements alone. However, it is clear that ULF wave amplitudes can still be seen on the ground, and so if they are involved in electron acceleration their energies cannot have been fully quenched. Specific case studies have shown that the periodicities of the fluctuations along the onset arc reside in the ~15–60 s period band [e.g., *Sakaguchi et al.*, 2009; *Rae et al.*, 2010] which also corresponds to the ULF wave period band which show large correlations with the growth of auroral intensity in this paper. As a result, we should conclude that if these ULF wave frequencies are observed by both ground magnetometers and all-sky imagers, then these waves could not have completely relinquished their energy to the auroral electron precipitation.

[30] Finally, we should note that any of these effects, either in the four main categories, or any of the sub-categories that we have discussed, should not necessarily be considered in isolation; that is, these considerations may be additive. For example, ULF waves may evolve in an inverse-cascade type manner, from small scale to larger-scales during onset and thus be largely screened from ground magnetometers [e.g., *Rae et al.*, 2009a, 2009b], but these waves may also precipitate electrons into the ionosphere [e.g., *Watt and Rankin*, 2010].

5. Conclusions

[31] In this paper, we demonstrate that the growth of auroral intensity and of ULF wave amplitudes is remarkably well correlated during auroral brightenings and substorms during these case studies. We show clearly that both wave amplitudes and auroral brightening experience similar periods of exponential growth that occur within essentially the same time frame surrounding the onset of a substorm. In two cases, it appears that the highest correlations between ULF wave amplitudes and auroral intensities as observed by the THEMIS ASIs are achieved when the magnetometer time series are shifted forward in time, i.e., ULF pulsations are correlated best with auroral intensities when the growth of pulsations occur prior to the growth of auroral intensification. During one event, however, the timing of the growth of auroral intensities and (most of the) ULF wave amplitudes are reversed, other than the 64 s period band, which still correlates best at large negative lags. However, it is not the relative timing of the magnetometer and ASI time series that is the subject of this paper. We therefore draw no conclusion on the relative timing of any time series with respect to any other time series in this paper, and highlight the new result that the ASI intensities and magnetometer pulsations are highly correlated during substorms and auroral brightenings.

[32] The highest correlations occur for timing lags that are close to the timing uncertainties involved in the wavelet analysis used herein. The lags are most likely close to zero. We conclude that the waves and particle precipitation are most likely physically linked at their source.

[33] We discuss four reasons for this high correlation: coincidence, instrumental effects, the response of the ionosphere to waves and precipitation, and finally, that the waves and auroral particles are physically linked at their source. We discount coincidence and instrumental effects as being primary causes for this relationship. We also conclude that ionospheric screening, while important, and most likely a contributing factor, cannot explain all of the results contained within this paper. In particular, small-amplitude ULF waves have been observed at the same time and at the same location as the first observable signatures of auroral onset [e.g., *Rae et al.*, 2009a, 2009b, 2010; *Walsh et al.*, 2010]. This leaves the possibility that the waves and particles are physically linked at their source as the most likely candidate. This testable hypothesis unsurprisingly requires the detailed observations of substorm onset using ground magnetometers and all-sky imagers, in conjunction with two satellites at differing altitudes along the nightside geomagnetic field, in a similar manner to that presented by *Dombeck et al.* [2005]. What that precise relationship entails is left to further study, but in this paper we demonstrate that ULF waves and auroral intensities should both be considered clear and interlinked proxies for the development of auroral intensifications and substorm onset.

[34] **Acknowledgments.** I.J.R., C.E.J.W., and L.G.O are funded by the Canadian Space Agency. K.R.M. is funded by Alberta Innovates. CARISMA is operated by the University of Alberta and funded by the Canadian Space Agency. We acknowledge NASA contract NAS5-02099 and V. Angelopoulos for use of data from the THEMIS Mission. The ground-based component of the THEMIS mission is funded by NSF award 1004736. We thank S. Mende and E. Donovan for use of the THEMIS ASI data and the CSA for logistical support in fielding and data retrieval from the GBO stations.

[35] Robert Lysak thanks the reviewers for their assistance in evaluating this paper.

References

Akasofu, S. I. (1964), The development of the auroral substorm, *Planet. Space Sci.*, *12*, 273–282, doi:10.1016/0032-0633(64)90151-5.

Akasofu, S. I. (1977), Magnetospheric substorms, *Q. J. R. Astron. Soc.*, *18*, 170–187.

Angelopoulos, V., et al. (2008), Tail reconnection triggering substorm onset, *Science*, *321*, 931–935, doi:10.1126/science.1160495.

Angelopoulos, V., et al. (2009), Response to comment on "Tail reconnection triggering substorm onset", *Science*, *324*, 1391.

Angenheister, G. (1913), Ueber die Fortpflanzungsgeschwindigkeit magnetischer Störungen und Pulsationen. Bericht über die erdmagnetischen Schnellregistierungen in Apia (Samoa), Batavia, Cheltenham, und Tsingtau im September 1911, *Nachr. Ges. Wiss. Goettingen, Math.-Phys. Kl.*, *1913*, 565–581.

Arnoldy, R. L., R. Rajashekar, L. J. Cahill, M. J. Engebretson, T. J. Rosenberg, and S. B. Mende (1987), Simultaneous measurement of aurora-related, irregular magnetic pulsations at northern and southern high latitudes, *J. Geophys. Res.*, *92*, 12,221–12,232, doi:10.1029/JA092iA11p12221.

Asamura, K., et al. (2009), Sheared flows and small-scale Alfven wave generation in the auroral acceleration region RID C-3460–2011, *Geophys. Res. Lett.*, *36*, L05105, doi:10.1029/2008GL036803.

Bösinger, T. (1989), On the spectral index of the Pi1b power spectrum, *Ann. Geophys.*, *7*, 375–386.

Bösinger, T., and A. G. Yahnin (1987), Pi1b type magnetic pulsation as a high time resolution monitor of substorm development, *Ann. Geophys., Ser. A*, *5*, 231–237.

Chaston, C., C. Carlson, R. Ergun, and J. McFadden (2000), Alfven waves, density cavities and electron acceleration observed from the FAST spacecraft, *Phys. Scr. T*, *84*, 64–68, doi:10.1238/Physica.Topical.084a00064.

Chaston, C., J. Bonnell, C. Carlson, M. Berthomier, L. Peticolas, I. Roth, J. McFadden, R. Ergun, and R. Strangeway (2002), Electron acceleration in the ionospheric Alfven resonator, *J. Geophys. Res.*, *107*(A11), 1413, doi:10.1029/2002JA009272.

Chi, P. J., C. T. Russell, and S. Ohtani (2009), Substorm onset timing via traveltime magnetoseismology, *Geophys. Res. Lett.*, *36*, L08107, doi:10.1029/2008GL036574.

Dombeck, J., C. Cattell, J. Wygant, A. Keiling, and J. Scudder (2005), Alfven waves and Poynting flux observed simultaneously by Polar and

FAST in the plasma sheet boundary layer, *J. Geophys. Res.*, *110*, A12S90, doi:10.1029/2005JA011269.
Donovan, E., et al. (2008), Simultaneous THEMIS in situ and auroral observations of a small substorm, *Geophys. Res. Lett.*, *35*, L17S18, doi:10.1029/2008GL033794.
Friedrich, E., J. C. Samson, I. Voronkov, and G. Rostoker (2001), Dynamics of the substorm expansive phase, *J. Geophys. Res.*, *106*, 13,145–13,163, doi:10.1029/2000JA000292.
Glassmeier, K. H., and H. Junginger (1987), Concerning the ionospheric modification of magnetospheric hydromagnetic waves: Case studies, *J. Geophys. Res.*, *92*(A11), 12,213–12,219, doi:10.1029/JA092iA11p12213.
Heppner, J. P. (1958), A study of the relationships between the aurora borealis and the geomagnetic disturbances caused by electric currents in the ionosphere, PhD thesis, Calif. Inst. of Technol., Pasadena.
Hughes, W., and D. Southwood (1976), Screening of micropulsation signals by atmosphere and ionosphere, *J. Geophys. Res.*, *81*, 3234–3240, doi:10.1029/JA081i019p03234.
Jacobs, J. A., S. Matsushita, Y. Kato, and V. A. Troitskaya (1964), Classification of geomagnetic micropulsations, *J. Geophys. Res.*, *69*, 180, doi:10.1029/JZ069i001p00180.
Kepko, L., and R. McPherron (2001), Comment on "Evaluation of low-latitude Pi2 pulsations as indicators of substorm onset using Polar ultraviolet imagery" by K. Liou, et al., *J. Geophys. Res.*, *106*, 18,919–18,922, doi:10.1029/2000JA000189.
Lester, M., W. Hughes, and H. Singer (1983), Polarization patterns of Pi 2 magnetic pulsations and the substorm current wedge, *J. Geophys. Res.*, *88*, 7958–7966, doi:10.1029/JA088iA10p07958.
Lester, M., J. A. Davies, and T. S. Virdi (1996), High-latitude Hall and Pedersen conductances during substorm activity in the SUNDIAL-ATLAS campaign, *J. Geophys. Res.*, *101*(A12), 26,719–26,728, doi:10.1029/96JA00979.
Liang, J., E. F. Donovan, W. W. Liu, B. Jackel, M. Syrjasuo, S. B. Mende, H. U. Frey, V. Angelopoulos, and M. Connors (2008), Intensification of preexisting auroral arc at substorm expansion phase onset: Wave-like disruption during the first tens of seconds, *Geophys. Res. Lett.*, *35*, L17S19, doi:10.1029/2008GL033666.
Liou, K., C. I. Meng, P. T. Newell, K. Takahashi, S. I. Ohtani, A. T. Y. Lui, M. Brittnacher, and G. Parks (2000), Evaluation of low-latitude Pi2 pulsations as indicators of substorm onset using Polar ultraviolet imagery, *J. Geophys. Res.*, *105*, 2495–2505, doi:10.1029/1999JA900416.
Liu, J., C. Gabrielse, V. Angelopoulos, N. A. Frissell, L. R. Lyons, J. P. McFadden, J. Bonnell, and K. H. Glassmeier (2011), Superposed epoch analysis of magnetotail flux transport during substorms observed by THEMIS, *J. Geophys. Res.*, *116*, A00I29, doi:10.1029/2010JA015886.
Liu, W. W., J. Liang, and E. F. Donovan (2008), Interaction between kinetic ballooning perturbation and thin current sheet: Quasi-electrostatic field, local onset, and global characteristics, *Geophys. Res. Lett.*, *35*, L20107, doi:10.1029/2008GL035757.
Lui, A. T. Y. (2009), Comment on "Tail reconnection triggering substorm onset", *Science*, *324*(5933), 1391, doi:10.1126/science.1167726.
Lysak, R. (1991), Feedback instability of the ionospheric resonant cavity, *J. Geophys. Res.*, *96*, 1553–1568, doi:10.1029/90JA02154.
Mann, I. R., et al. (2008), The Upgraded CARISMA Magnetometer Array in the THEMIS Era, *Space Sci. Rev.*, *141*, 413–451, doi:10.1007/s11214-008-9457-6.
McPherron, R. L., C. W. Arthur, M. D. Bossen, and C. T. Russell (1973), Micropulsation substorm at synchronous orbit Ats-1 observations of ULF waves, *Trans. AGU*, *54*, 420.
Mende, S., C. Carlson, H. Frey, T. Immel, and J. Gerard (2003), IMAGE FUV and in situ FAST particle observations of substorm aurorae, *J. Geophys. Res.*, *108*(A4), 8010, doi:10.1029/2002JA009413.
Mende, S. B., S. E. Harris, H. U. Frey, V. Angelopoulos, C. T. Russell, E. Donovan, B. Jackel, M. Greffen, and L. M. Peticolas (2008), The THEMIS array of ground-based observatories for the study of auroral substorms, *Space Sci. Rev.*, *141*, 357–387, doi:10.1007/s11214-008-9380-x.
Mende, S. B., H. U. Frey, V. Angelopoulos, and Y. Nishimura (2011), Substorm triggering by poleward boundary intensification and related equatorward propagation, *J. Geophys. Res.*, *116*, A00I31, doi:10.1029/2010JA015733.
Milling, D. K., I. J. Rae, I. R. Mann, K. R. Murphy, A. Kale, C. T. Russell, V. Angelopoulos, and S. Mende (2008), Ionospheric localisation and expansion of long-period Pi1 pulsations at substorm onset, *Geophys. Res. Lett.*, *35*, L17S20, doi:10.1029/2008GL033672.
Murphy, K. R., I. J. Rae, I. R. Mann, D. K. Milling, C. E. J. Watt, L. Ozeke, H. U. Frey, V. Angelopoulos, and C. T. Russell (2009a), Wavelet-based ULF wave diagnosis of substorm expansion phase onset, *J. Geophys. Res.*, *114*, A00C16, doi:10.1029/2008JA013548.
Murphy, K. R., I. J. Rae, I. R. Mann, A. P. Walsh, D. K. Milling, C. E. J. Watt, L. Ozeke, H. U. Frey, V. Angelopoulos, and C. T. Russell (2009b), Reply to comment by K. Liou and Y.-L. Zhang on "Wavelet-based ULF wave diagnosis of substorm expansion phase onset", *J. Geophys. Res.*, *114*, A10207, doi:10.1029/2009JA014351.
Newell, P. T., A. R. Lee, K. Liou, S. I. Ohtani, T. Sotirellis, and S. Wing (2010), Substorm cycle dependence of various types of aurora, *J. Geophys. Res.*, *115*, A09226, doi:10.1029/2010JA015331.
Newton, R., D. Southwood, and W. Hughes (1978), Damping of geomagnetic pulsations by ionosphere, *Planet. Space Sci.*, *26*, 201–209, doi:10.1016/0032-0633(78)90085-5.
Nishimura, Y., L. Lyons, S. Zou, V. Angelopoulos, and S. Mende (2010), Substorm triggering by new plasma intrusion: THEMIS all-sky imager observations, *J. Geophys. Res.*, *115*, A07222, doi:10.1029/2009JA015166.
Peñano, J., and G. Ganguli (2000), Generation of ELF electromagnetic waves in the ionosphere by localized transverse dc electric fields: Subcyclotron frequency regime, *J. Geophys. Res.*, *105*, 7441–7457, doi:10.1029/1999JA000303.
Rae, I. J., et al. (2009a), Near-Earth initiation of a terrestrial substorm, *J. Geophys. Res.*, *114*, A07220, doi:10.1029/2008JA013771.
Rae, I. J., et al. (2009b), Timing and localization of ionospheric signatures associated with substorm expansion phase onset, *J. Geophys. Res.*, *114*, A00C09, doi:10.1029/2008JA013559.
Rae, I. J., C. E. J. Watt, I. R. Mann, K. R. Murphy, J. C. Samson, K. Kabin, and V. Angelopoulos (2010), Optical characterisation of the growth and spatial structure of a substorm onset arc, *J. Geophys. Res.*, *115*, A10222, doi:10.1029/2010JA015376.
Rae, I. J., K. R. Murphy, C. E. J. Watt, and I. R. Mann (2011), On the nature of ULF wave power during nightside auroral activations and substorms: 2. Temporal evolution, *J. Geophys. Res.*, *116*, A00I22, doi:10.1029/2010JA015762.
Saito, T. (1969), Geomagnetic pulsations, *Space Sci. Rev.*, *10*, 319, doi:10.1007/BF00203620.
Sakaguchi, K., K. Shiokawa, A. Ieda, R. Nomura, A. Nakajima, M. Greffen, E. Donovan, I. R. Mann, H. Kim, and M. Lessard (2009), Fine structures and dynamics in auroral initial brightening at substorm onsets, *Ann. Geophys.*, *27*, 623–630, doi:10.5194/angeo-27-623-2009.
Shay, M. A., J. F. Drake, J. P. Eastwood, and T. D. Phan (2011), Super-Alfvelnic propagation of substorm reconnection signatures and Poynting flux, *Phys. Rev. Lett.*, *107*, 065001, doi:10.1103/PhysRevLett.107.065001.
Smith, A., M. Freeman, S. Hunter, and D. Milling (2002), VLF, magnetic bay, and Pi2 substorm signatures at auroral and midlatitude ground stations, *J. Geophys. Res.*, *107*(A12), 1439, doi:10.1029/2002JA009389.
Takahashi, K., and K. Liou (2004), Longitudinal structure of low-latitude Pi2 pulsations and its dependence on aurora, *J. Geophys. Res.*, *109*, A12206, doi:10.1029/2004JA010580.
Uozumi, T., K. Yumoto, H. Kawano, A. Yoshikawa, J. V. Olson, S. I. Solovyev, and E. F. Vershinin (2000), Characteristics of energy transfer of Pi 2 magnetic pulsations: Latitudinal dependence, *Geophys. Res. Lett.*, *27*(11), 1619–1622, doi:10.1029/1999GL010767.
Voronkov, I., R. Rankin, P. Frycz, V. T. Tikhonchuk, and J. C. Samson (1997), Coupling of shear flow and pressure gradient instabilities, *J. Geophys. Res.*, *102*, 9639–9650, doi:10.1029/97JA00386.
Walsh, A. P., et al. (2010), Comprehensive ground-based and in-situ observations of substorm expansion phase onset, *J. Geophys. Res.*, *115*, A00I13, doi:10.1029/2010JA015748.
Watt, C. E. J., and R. Rankin (2009), Electron trapping in shear Alfven waves that power the aurora, *Phys. Rev. Lett.*, *102*, 045002, doi:10.1103/PhysRevLett.102.045002.
Watt, C. E. J., and R. Rankin (2010), Do magnetospheric shear Alfven waves generate sufficient electron energy flux to power the aurora?, *J. Geophys. Res.*, *115*, A07224, doi:10.1029/2009JA015185.
Watt, C. E. J., R. Rankin, I. J. Rae, and D. M. Wright (2005), Self-consistent electron acceleration due to inertial Alfvén wave pulses, *J. Geophys. Res.*, *110*, A10S07, doi:10.1029/2004JA010877.
Wu, K., and C. Seyler (2003), Instability of inertial Alfven waves in transverse sheared flow, *J. Geophys. Res.*, *108*(A6), 1236, doi:10.1029/2002JA009631.
Wygant, J., et al. (2002), Evidence for kinetic Alfven waves and parallel electron energization at 4–6 R-E altitudes in the plasma sheet boundary layer, *J. Geophys. Res.*, *107*(A8), 1201, doi:10.1029/2001JA900113.
Yoshikawa, A., and M. Itonaga (2000), The nature of reflection and mode conversion of MHD waves in the inductive ionosphere: Multistep mode conversion between divergent and rotational electric fields, *J. Geophys. Res.*, *105*(A5), 10,565–10,584, doi:10.1029/1999JA000159.